Published in final edited form as:
Cryst Growth Des. 2009 June 3; 9(6): 2566–2569. doi:10.1021/cg900289d.

Microfluidic Generation of Lipidic Mesophases for Membrane Protein Crystallization

Sarah L. Perry[†], **Griffin W. Roberts**[†], **Joshua D. Tice**[†], **Robert B. Gennis**[‡], and **Paul J. A. Kenis**[†,*]

[†] Department of Chemical & Biomolecular Engineering, University of Illinois at Urbana-Champaign, 600 South Mathews Avenue, Urbana, Illinois 61801, USA

[‡] Department of Biochemistry, University of Illinois at Urbana-Champaign, 600 South Mathews Avenue, Urbana, Illinois 61801, USA

Abstract

We report on a microfluidic method for the formation of aqueous/lipid mesophases to enable screening of suitable crystallization conditions of membrane proteins from a membrane-like phase in sub-20 nanoliter volumes. This integrated microfluidic chip and the employed mixing strategy address the specific challenges associated with the mixing of fluids of highly different viscosities (here a factor of 30) as well as the non-Newtonian character of the resulting mesophases. The chip requires less than 20 nL of material per condition screened whereas typically on the order of 10 μL or more is needed for a batch preparation in the present screening methods. We validated our approach with the successful crystallization of the membrane protein bacteriorhodopsin.

This communication reports on a method for the formation of aqueous/lipid mesophases at the sub-20 nanoliter level to enable screening for suitable *in-meso* (lipidic cubic phase or LCP) crystallization conditions for membrane proteins. Membrane proteins are critical components of many fundamental biological processes, enabling cell signaling and material and energy transduction across cellular boundaries.[1] As such, their malfunction has been linked to numerous diseases and they are common targets for pharmacological treatments.2 However, an understanding of the mechanisms whereby these proteins operate and attempts at rational drug design have been limited by difficulties in obtaining high resolution structural information on these proteins.

A key bottleneck in the determination of membrane protein structures is the identification of appropriate crystallization conditions. Membrane proteins are typically available in quantities that are insufficient to screen a large number of conditions.3 Additionally, they exhibit poor solubility due to their amphiphilic nature.1,[4] As a result, a tremendous disparity has developed between the number of known structures for membrane proteins (432) as compared to soluble, globular proteins (>56,000).[5,6]

In recent years, microfluidic technology has been successfully utilized for high throughput screening of crystallization conditions at the sub-nanoliter scale.[3,7] Thus far crystallization of membrane proteins in microfluidic systems has been limited to *in-surfo* methods where

Department of Chemical & Biomolecular Engineering, University of Illinois at Urbana-Champaign, Address: 600 S. Mathews Ave., Urbana, IL 61801, Phone: (217) 265-0523, Fax: (217) 333-5052, Email: kenis@illinois.edu, Web Address: http://www.scs.uiuc.edu/~pkgroup/.

Supporting Information Available. Details of the mixing sequence and setup of the crystallization trials, including injection of precipitant are available free of charge via the Internet at http://pubs.acs.org.

detergents are used to solubilize membrane proteins and crystallization is attempted as for soluble proteins.[3,8]

The *in-meso* crystallization method is an alternative to the *in-surfo* method. It uses an artificial aqueous/lipid mesophase to maintain membrane proteins in a membrane-like environment.[1,4] This method exploits the complex phase behavior of aqueous/lipid systems (e.g. lamellar, bicontinuous cubic phases),[9,10] creating local variations in the curvature of the lipid bilayers to drive crystal nucleation and growth.[1,4,10–13] Despite its benefits, implementation of the *in-meso* approach to crystallization on the microscale has been particularly difficult because of the challenges associated with mixing fluids of vastly different viscosities. Thus far, the aqueous/lipid mesophases necessary for the *in-meso* approach have been prepared either by centrifugation12 or using coupled microsyringes.[14] Unfortunately the preparative scale of both of these methods requires the creation of relatively large amounts of mesophase (10–500 μL) due to the scale at which mixing can be performed.

While many microfluidic strategies for mixing have been reported,[15,16] they are limited to the mixing of fluids both of similar and relatively low viscosities, such as two aqueous solutions. The viscosities of the solutions to be mixed here differ by a factor of ~30; 2.45×10^{-2} Pa-s for the monoolein lipid phase (1-monooleoyl-*rac*-glycerol, Fluka), versus 7.98×10^{-4} Pa-s for the aqueous phase. Furthermore, the resulting mesophase has a viscosity that is a factor of $\sim10^5$ larger (~48.3 Pa-s at a shear rate of 71.4 s^{-1}) than the viscosity of the aqueous phase. Moreover, the resulting mixture exhibits highly non-Newtonian behavior.[17,18] The highly viscous and non-Newtonian nature of the fluids render previously reported microfluidic mixing approaches ineffective.

The pressure required to move increasingly viscous fluids through a channel of set dimensions scales with viscosity. In microfluidic chips where flow is driven by the actuation of pneumatic valves, the maximum achievable pressure is limited by the actuation pressure supplied to the valves, which in turn limits the viscosity a fluid can have to be used in a given microfluidic network. To still be able to pump fluids of high viscosities, e.g. the lipids used here, an adjustment of channel dimensions, specifically the reduction of channel length and/or enlargement of the cross-sectional area, can overcome pressure limitations. Additionally, non-Newtonian fluid behavior, such as the viscoelastic properties of the lipidic mesophases created here, needs to be accounted for. For pneumatic pumping to be effective, the rate of individual valve actuation needs to be reduced to a timescale longer than the timescale of viscoelastic relaxation present in the fluid. Otherwise the fluid will deform and bounce back elastically as opposed to actual flow.

Here we report an integrated microfluidic chip (Figure 1) capable of mixing lipids with aqueous solutions to enable sub-microliter screening for crystallization conditions *in-meso*. We employ the principles of chaotic mixing via time-periodic flow in a tendril-whorl fashion to prepare homogeneous aqueous/lipid mesophases.[19] Each experiment consumes less than 20 nL of material with the potential to scale down further to the 0.1 nL level. We validate our approach by the successful *in-meso* crystallization of the well-characterized membrane protein bacteriorhodopsin.[1,4,12,13,20]

The microfluidic chip was fabricated out of polydimethylsiloxane (PDMS, General Electric RTV 650) bonded to a glass substrate using standard multi-layer soft lithographic procedures reported previously.[7,21] We designed and fabricated a microfluidic chip capable of metering and mixing solutions followed by crystallization (Figure 1). Fluid flow in the bottom, fluid layer is controlled pneumatically. Isolation valves (black) over lines connecting the various chambers are used to control the direction of fluid flow while injection valves located over each fluid chamber (purple, blue, and orange) are used to drive the movement of material from

one chamber into the next. The short length of the injection lines between fluid chambers as well as the larger size of the fluid chambers compared to the injection lines allow for the pumping of highly viscous and non-Newtonian fluids. Protein solution and lipid are introduced into the side (4.9 nL each) and center chambers (9.6 nL), respectively (Figure 2a), displacing air, which escapes by permeation through the PDMS. In the present configuration some additional volume is lost in the supply lines and inlets (~40%), but this design has not been optimized. Furthermore, the relative losses within a chip will decrease as the number of mixing and crystallization units per chip is scaled out.

The mixing chambers are designed to produce different types of fluid motion on two scales of operation. At the larger scale of fluid flow between chambers, flow proceeds alternately in a linear fashion from the side chambers to the center chamber through all of the available injection lines (Figure 2b), and then by two recirculating loops that utilize one injection line for flow directed into the side chambers and the remaining two lines to return to the center chamber (Figure 2c–e). These two motions are used to avoid issues associated with the reversibility of laminar flow. The asymmetric arrangement of the side chambers enables offset fluid injection into the center chamber. The rounded chambers also reduce dead volume (fluid not involved in mixing). Additionally, the injection lines between chambers only represent a short distance over which the pressure drop in the fluid is dissipated, thus avoiding further difficulties associated with moving highly viscous fluids over long distances. A complete mixing cycle is composed of a sequence of 12 different valve actuations (see supporting information). These steps are actuated with equal spacing at a total cycle speed in the range of 5 to 25 s/cycle.

Each point of injection leads to mixing by tendril-whorl type flow (Figure 3).[19] In this manner chaotic mixing is done by stretching and folding the two fluid components until the length-scale of the individual fluid lamellae is on the order of the diffusion length. Tendril-type flow occurs as the fluid stretches upon moving from one fluid chamber to another through a narrow injection channel (Figure 3c). Whorl-type flow occurs as fluid leaves the injection channel and enters a fluid chamber where it then folds around in an eddy-like fashion (Figure 3b). This whorl motion is further enhanced when fluid enters a chamber from multiple injection lines. Birefringence (or the lack thereof) was used to visualize the extent of mixing in the chip.[12] The aqueous/lipid mixture was observed to be homogeneous and mostly non-birefringent within 1–2 min. of mixing (Figure 2f), indicating the formation of the desired cubic phase.

After mixing is complete, the mesophase is transferred to a crystallization chamber via actuation of the chamber valves. The side chambers are first emptied into the center chamber (Figure 4a1) and then the center chamber valve is used to drive the entire bolus into a single crystallization chamber of defined geometry (Figure 4a2). A specific amount of a precipitant solution, e.g. 2.5M Sørenson phosphate buffer, can then be injected from the precipitant chamber (see supporting information). Alternatively, a chip where a large well has been punched through the PDMS over the crystallization chamber can be used for crystallization trials to facilitate harvesting of crystals (Figure 4a). In this punched-hole chip the precipitant solution is pipetted directly into the well prior to preparation of the mesophase and the well is sealed with Crystal Clear tape (Hampton Research) for the duration of the crystallization experiment. The size of this precipitant reservoir is large enough that evaporative losses through the PDMS would be insignificant over the course of an experiment.

As a proof-of-concept, we performed *in-meso* crystallization of the membrane protein bacteriorhodopsin using this chip. A precipitant solution of 2.5M Sørenson phosphate buffer at pH 5.5 was pipetted into the precipitant reservoir and sealed. The lipid monoolein and a solution of bacteriorhodopsin (13.5 mg/mL solubilized in 25 mM NaH_2PO_4 (EMD Chemicals Inc.) with 1.2% w/v octyl β-D-glucopyranoside (Anatrace), pH 5.5) were then mixed into a

homogeneous mesophase (Figure 2f). The resulting bolus of mesophase was then moved from the mixing chambers to the crystallization chamber by actuation of valves (Figure 4a). Finally the entire chip was sealed with Crystal Clear tape and stored in the dark at room temperature. Plate-like purple hexagonal crystals appeared within a few days (Figure 4b) and grew to a diameter of 20–50 μm, comparable with dimensions reported in the literature.[1,4]

In conclusion, a microfluidic chip for the on-chip formation of lipidic mesophases for *in-meso* crystallization at volumes sub-20 nanoliter has been demonstrated. This achievement is particularly significant due to the challenges of not only mixing fluids of different viscosities, but also driving fluid flow of highly viscous materials on the microfluidic scale. The feasibility of *in-meso* membrane protein crystallization was then validated using the membrane protein bacteriorhodopsin. Compared to the present *in-meso* crystallization screening approaches, the operational scale and amenability for high throughput processing of the microfluidic approach introduced here allows for a 1000-fold decrease in the preparative scale at which the mixing necessary for mesophase formulation can be performed. This capability is particularly necessary to extend crystallization screening for the *in-meso* technique to include multiple lipids and/or different lipid compositions. In addition to crystallization screening, the ability to set up a large number of trials will allow detailed study of the interactions between artificial mesophases, membrane proteins, and precipitating agents. Better understanding of these interactions will facilitate the rational design of sparse matrix crystallization screens geared to determine suitable *in-meso* crystallization conditions for membrane proteins of unknown structure.[1,10]

Supplementary Material

Refer to Web version on PubMed Central for supplementary material.

Acknowledgments

This work was funded through the NIH Roadmap for Medical Research (R21 GM075930-01) a NIH Kirschstein Predoctoral Fellowship (F31 EB008330) and a critical research initiative grant (Campus Research Board, UIUC). We thank Prof. S. Sligar and Dr. T. Baybert, as well as Prof. C. Rienstra and Dr. D. Berthold for the bacteriorhodopsin samples, Dr. A. Vakkasoglu for FTIR work, and Prof. J.J.L. Higdon for helpful discussions.

References

1. Landau EM, Rosenbusch JP. P Natl Acad Sci USA 1996;93:14532–14535.
2. Quick M, Javitch JA. Proceedings of the National Academy of Sciences of the United States of America 2007;104:3603–3608. [PubMed: 17360689]
3. Li L, Mustafi D, Fu Q, Tereshko V, Chen DLL, Tice JD, Ismagilov RF. Proceedings of the National Academy of Sciences of the United States of America 2006;103:19243–19248. [PubMed: 17159147]
4. Rummel G, Hardmeyer A, Widmer C, Chiu ML, Nollert P, Locher KP, Pedruzzi I, Landau EM, Rosenbusch JP. Journal of Structural Biology 1998;121:82–91. [PubMed: 9618339]
5. Membrane Proteins of Known 3D Structure. [accessed Mar. 9, 2009]. http://blanco.biomol.uci.edu/Membrane_Proteins_xtal.html
6. RCSB Protein Data Bank. http://www.rcsb.org/ (accessed Jan. 9, 2009).
7. Hansen CL, Skordalakes E, Berger JM, Quake SR. Proceedings of the National Academy of Sciences of the United States of America 2002;99:16531–16536. [PubMed: 12486223]
8. Sommer MOA, Larsen S. Journal of Synchrotron Radiation 2005;12:779–785. [PubMed: 16239748]
9. Briggs J, Chung H, Caffrey M. Journal De Physique Ii 1996;6:723–751.
10. Cherezov V, Fersi H, Caffrey M. Biophysical Journal 2001;81:225–242. [PubMed: 11423409]
11. Grabe M, Neu J, Oster G, Nollert P. Biophysical Journal 2003;84:854–868. [PubMed: 12547769]
12. Nollert P. Methods 2004;34:348–353. [PubMed: 15325652]

13. Caffrey M. Journal of Structural Biology 2003;142:108–132. [PubMed: 12718924]
14. Cheng AH, Hummel B, Qiu H, Caffrey M. Chemistry and Physics of Lipids 1998;95:11–21. [PubMed: 9807807]
15. Hansen CL, Sommer MOA, Quake SR. Proceedings of the National Academy of Sciences of the United States of America 2004;101:14431–14436. [PubMed: 15452343]
16. Stroock AD, Dertinger SKW, Ajdari A, Mezic I, Stone HA, Whitesides GM. Science 2002;295:647–651. [PubMed: 11809963]
17. Bonacucina G, Palmieri GF, Craig DQM. Journal of Pharmaceutical Sciences 2005;94:2452–2462. [PubMed: 16200546]
18. Mezzenga R, Meyer C, Servais C, Romoscanu AI, Sagalowicz L, Hayward RC. Langmuir 2005;21:3322–3333. [PubMed: 15807570]
19. Ottino, JM. The kinematics of mixing: stretching, chaos, and transport. Cambridge University Press; 1989.
20. Luecke H, Schobert B, Richter HT, Cartailler JP, Lanyi JK. J Mol Biol 1999;291:899–911. [PubMed: 10452895]
21. Unger MA, Chou HP, Thorsen T, Scherer A, Quake SR. Science 2000;288:113–116. [PubMed: 10753110]

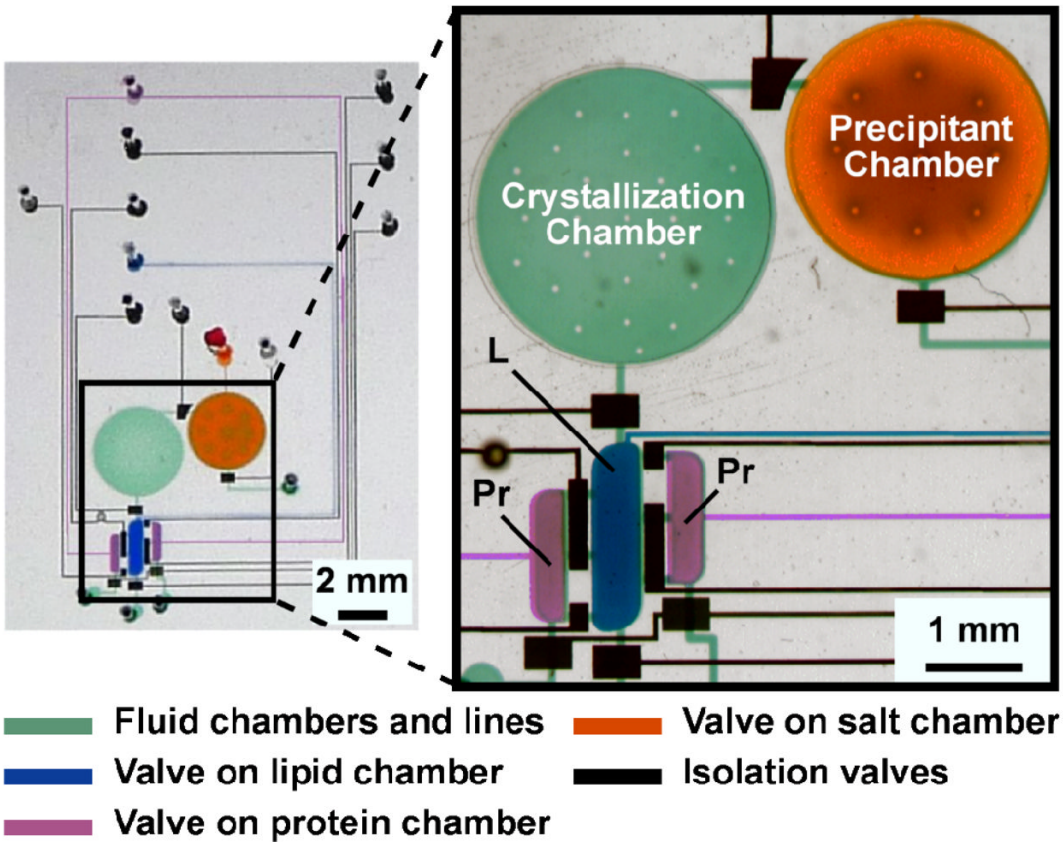

Figure 1.

Optical micrograph of a microfluidic chip capable of mixing lipids (L) and aqueous protein (Pr) solutions by pneumatic actuation of the isolation valves (black) between the chambers and the injection valves (purple and blue) on top of the three large chambers (2-Pr, L). Crystallization occurs in a separate crystallization chamber where the mesophase is combined with a precipitant solution that is introduced from a separate circular chamber at the top. The fluidic layer is filled with a green solution and is partially covered by various valves (purple, blue, black, orange) in the control layer.

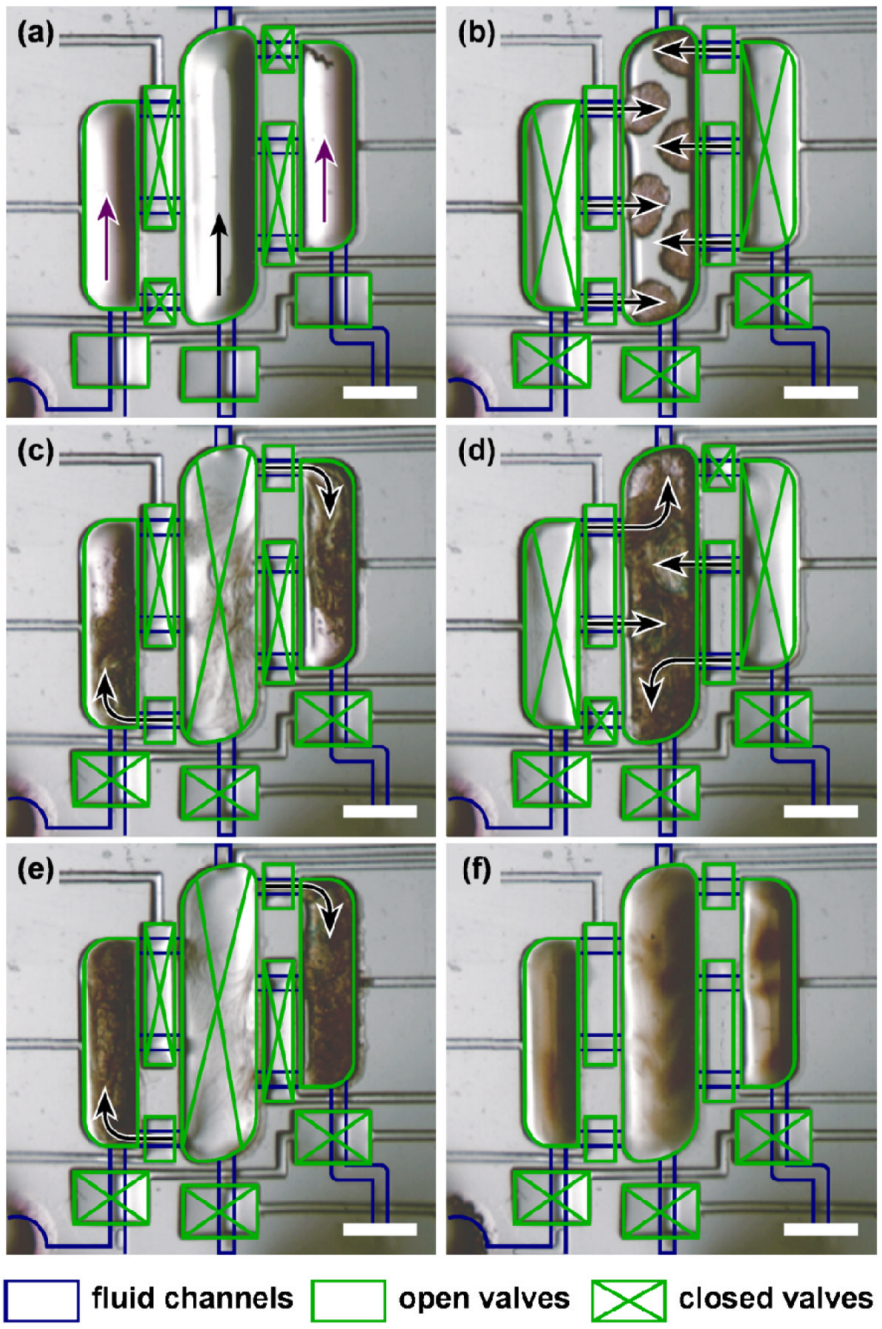

Figure 2.

Optical micrographs of an aqueous 13.5 mg/mL bacteriorhodopsin solution (left and right chambers) being mixed with the lipid monoolein (center chamber) in a microfluidic chip. The blue lines delineate the edges of the fluidic channels. (a) Filling of chambers with protein solution and lipid through inlet channels (arrows); (b) Straight-line injection of protein into the lipid-containing center chamber; (c–e) Consecutive, chamber-to-chamber injection of the fluid mixture through different sets of inlets to create a net circulatory motion. The mixing cycle then repeats starting at (b). (f) The slightly birefringent mixture (observed through partially crossed polarizers) after 1 min. of mixing. Scale bars: 500 μm.

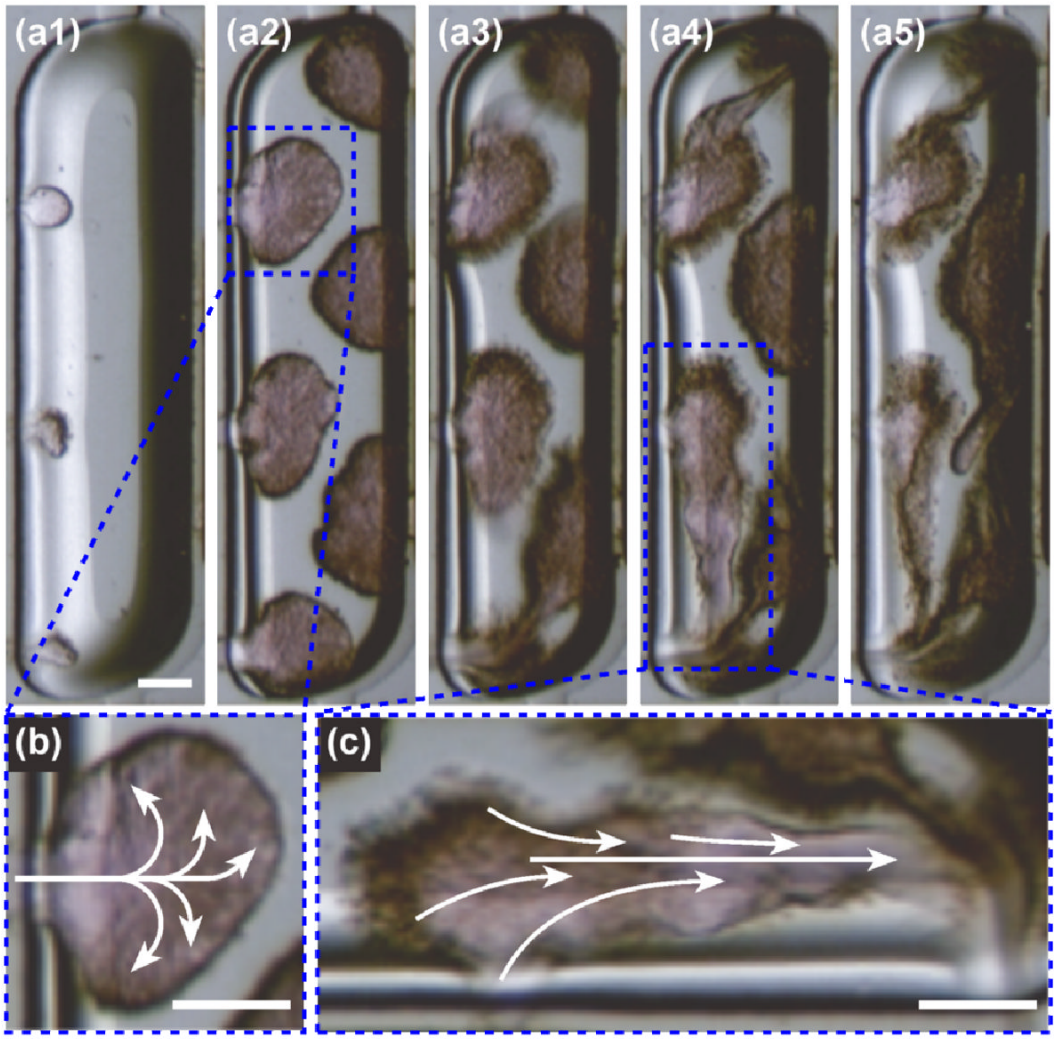

Figure 3.
Optical micrographs of an aqueous 13.5 mg/mL bacteriorhodopsin solution being mixed with the lipid monoolein in the center chamber of a microfluidic chip. (a1–a5) Injection of protein solution into the lipid such that tendril-whorl flow occurs; (b) Eddying (whorl) flow within the injected protein solution indicated by divergent arrows; (c) Stretching (tendril) flow, indicated by convergent arrows, as the contents of the center chamber are pushed through a the narrow injection line. Scale bars: 150 μm.

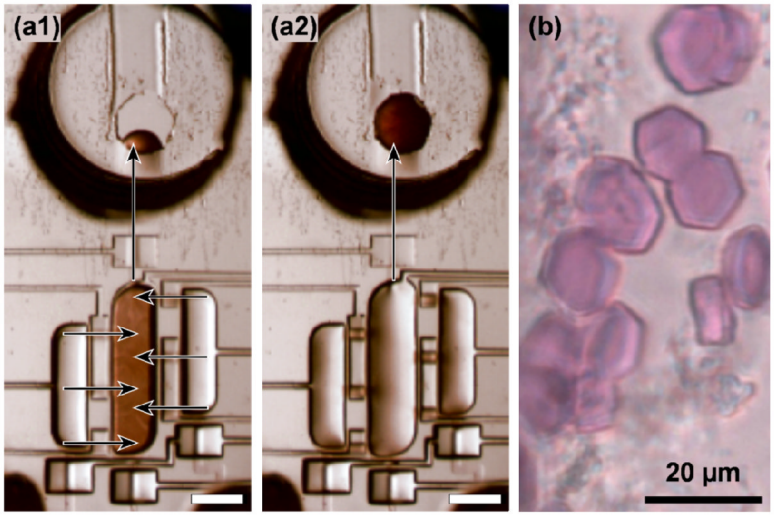

Figure 4.
(a) Optical micrographs of a homogeneous mesophase of 13.5 mg/mL bacteriorhodopsin solution and monoolein being moved from the mixing chambers into the crystallization chamber in a punched-hole chip by actuation of the mixing chamber valves. Scale bar: 500 μm. (b) Optical micrograph of the resulting bacteriorhodopsin crystals grown on-chip via the *in-meso* method.